

Activated gallic acid as radical and oxygen scavenger in biodegradable packaging film

Fabio di Giuseppe^a, Fanny Coffigniez^{b,*}, Chahinez Aouf^b, Valérie Guillard^b, Elena Torrieri^a

^a Department of Agricultural Sciences, University of Naples "Federico II", Via Università 100, 80055 Portici, NA, Italy

^b IATE, Agro polymers Engineering & Emerging Technology, Univ Montpellier, INRAE, Institut Agro, Montpellier & CIRAD, Montpellier, France

ARTICLE INFO

Keywords:

Active packaging
Biodegradable polymer
O₂ scavenger
Antiradical
O₂ scavenging modelling

ABSTRACT

A coupled experimental and modelling approach was developed to characterize the radical inhibition and oxygen scavenger properties of gallic acid/ sodium carbonate mixture included in a PHBV film. PHBV active packaging was produced by thermoforming. In contact with aqueous and fatty food simulants, almost 30% of the initial gallic acid was released into food simulants A (10% ethanol), and D1 (50% ethanol), where it showed a radical inhibition value (I%) reaching $68 \pm 0.1\%$ and $77 \pm 0.1\%$ respectively, while no release was observed in food simulant D2 (isooctane). In addition, the active films displayed an O₂ scavenger capacity of 120 mg O₂ g⁻¹ GA at room temperature, after 10 days of storage. Models showed a good fitting to experimental data. The PHBV active packaging combining both antiradical and oxygen scavenger activities has high potential for food protection. However, some improvements are still needed to enhance its oxygen barrier capacity and to meet the regulation.

1. Introduction

Nowadays, one major challenge is to develop a sustainable packaging with low environmental impact, able to preserve food quality and safety. The use of biobased and biodegradable packaging is a way to reduce both the exploitation of fossil resources and the accumulation of plastic waste, thus preventing the environmental and health problems that result from this (Cazón, Velazquez, Ramírez, & Vázquez, 2017; Guillard et al. 2018; Mohamed, El-Sakhawy, & El-Sakhawy, 2020).

In addition, this biodegradable packaging should also be able to preserve the quality of food and extend its shelf life in order to reduce food waste and prevent food-borne diseases (Angellier-Coussy, Guillard, Guillaume, & Gontard, 2013; Coffigniez, Matar, Gaucel, Gontard, & Guilbert, 2021). Oxidation is one of the major food degradations. It is responsible for structural alterations, producing off-flavors, discoloration and loss of nutritional quality and safety due to the formation of potentially toxic secondary compounds (lipid and protein oxidation), thus making foods unsuitable for consumption (Gómez-Estaca, López-de-Dicastillo, Hernández-Muñoz, Catalá, & Gavara, 2014; Hellwig, 2019). One way to limit these oxidation reactions is the use of active packaging containing antioxidants that can diffuse into the food or act as oxygen absorbers by maintaining an oxygen-free atmosphere

(Vermeiren, Devlieghere, Van Beest, De Kruijf, & Debevere, 1999).

To be used in food packaging, antioxidants should meet certain criteria. They have to (i) be safe; (ii) effective at low concentrations and (iii) not modify odor, color and flavor of the product and (iv) above all, should comply with food and packaging regulation into force. Due to their good antioxidant activity, natural phenolic compounds seem to be ideal candidates for integration into a fully biobased and biodegradable system (Sanches-Silva et al., 2014). Different studies dealing with the incorporation of phenolic compounds into biobased films to extend the food shelf life have been reported (Carrizo, Taborda, Nerin, & Bosetti, 2016; Licciardello, Wittenauer, Saengerlaub, Reinelt, & Stramm, 2015; Radi, Firouzi, Akhavan, & Amiri, 2017; Wang et al., 2019).

Gallic acid (2,3,4-trihydroxybenzoic acid) (GA), a phenolic acid present in different parts of superior plants such as bark, wood, leaf, root and seed (Campo, Pinelli, & Romani, 2016; Luzi et al., 2019) has the particularity of having three phenolic hydroxyl groups in the ortho position, which increases its antioxidant activity. By means of electrospinning, GA was encapsulated into lentil flour/polyethylene oxide and methylcellulose/polyethylene oxide nanofibers. Due to the release of GA into walnuts, the resulting materials led to the decrease of their peroxide value by half at 40 °C for 21 days of storage (Aydogdu et al. 2019).

The oxygen scavenging ability of GA was investigated by Ahn,

* Correspondence to: IATE, 2 place Pierre Viala, Bat 31, 34060 Montpellier, France.

E-mail address: France.fanny.coffigniez@umontpellier.fr (F. Coffigniez).

<https://doi.org/10.1016/j.fpsl.2022.100811>

Received 6 July 2021; Received in revised form 2 December 2021; Accepted 13 January 2022

Available online 20 January 2022

2214-2894/© 2022 Elsevier Ltd. All rights reserved.

Gaikwad, and Lee (2016); Pant, Sangerlaub, and Muller (2017) ; Singh, Singh, Kumar, and Gaikwad (2020) and Wanner (2010) who showed that GA combined to alkaline molecules (sodium carbonate, sodium hydroxide or potassium chloride) had a strong oxygen absorption capacity when it was incorporated in low density polyethylene film; bio-based multilayer film and chitosan film respectively. In the presence of a base, the oxygen scavenger activity of gallic acid is activated by humidity derived from the product or the environment. Indeed, GA is a weak polyprotic acid with four acidic protons. As a function of the medium pH, different gallate anions can be formed. In the presence of dissolved oxygen, the autooxidation mechanism gives rise to gallate radicals by electron transfer or hydrogen atom transfer. This process leads to the formation of several GA autooxidation intermediates, along with the absorption of oxygen (Pant, Ozkasikci, Furtauer, & Reinelt, 2019; Wanner, 2010). Accurate determination of the O₂ absorption capacity and absorption rate is a prerequisite to modelling approach of the oxygen diffusion – reaction in material containing antioxidants. Modelling of such activity is important to design efficient system well targeted to the intended application as food packaging, as it was previously applied on iron based scavenging films for instance (Kombaya-Touckia-Linin et al. 2019). However, this approach was never carried out on gallic acid based scavenging films.

Poly(3-hydroxybutyrate-co-3-hydroxyvalerate) commonly known as PHBV is a biobased polyester belonging to the wide family of polyhydroxyalkanoate polymers. It displays good barrier properties and its physical properties are similar to some fossil-derived polymers such as polypropylene. Furthermore, it is non toxic, biocompatible and biodegradable in natural conditions (Berthet et al. 2015; Bossu et al. 2020). To the best of our knowledge, the design of an active packaging based on the PHBV/GA system, which could combine oxygen scavenging (by absorbing atmospheric oxygen) and radical scavenging (by migrating into food) activities, has never been studied before.

In the present work, PHBV film containing 5 wt% of activated GA was produced. The antioxidant activity of GA as both radical and oxygen scavenger was deeply investigated and a diffusion-reaction mathematical model was applied to predict the oxygen scavenger activity of the active packaging. This is the first time that such complete experimental and modelling approach was carried out on GA-based material targeting both antioxidant and oxygen scavenger activities.

2. Materials and methods

2.1. Materials

Gallic acid monohydrate (GA) and sodium carbonate (Na₂CO₃) were purchased from abcr GmbH and Geyer (Germany) respectively. Tianan (China) commercial grades of poly (3-hydroxybutyrate-co-3-hydroxyvalerate) with 3 wt% of 3HV (P(3HB-co-3HV)) in the form of pure uncompound powder with no additive, was purchased from Natureplast (France). Ultrapure water was obtained from a Millipore Milli-Q system (Millipore, Bedford, MA, USA). 2,2-diphenyl-1-picryl-hydrazyl radical (DPPH), ethanol 96%, methanol 99%, formic acid 96%, acetonitrile 99.9% and isooctane (for synthesis) were purchased from Sigma Aldrich France.

2.2. Preparation of the active film: compounding and thermoforming

PHBV, GA and Na₂CO₃ powders were separately dried at 60 °C for at least 48 h before using. PHBV powder containing 5% (w/w) of GA and 2.5% (w/w) of Na₂CO₃ (weight ratio of 2:1) was mixed and melt-blended using a co-rotating twin-screw microextruder (model “process 11” thermofisher). The screw speed was set at 200 rpm and the barrel temperature profile to 180 °C (from top to bottom). The residence time was 1.5 min. The melt strain was cooled down at room temperature (and air conditions) and pelletized (Pelletizer from Thermofischer, Germany). After drying during one night at 60 °C under vacuum, the

pellets were transformed into films by means of an hydraulic thermo-press (CFM 20 T, Pinette Emidecau Industries, Chalon sur Saone cedex, France) at 180 °C. Pellets were melt for 1 min at 5 bar, then 1 min at 150 bar. The film was cooled down using a cold bath water on the surface of the metal form used to produce the films (in air conditions). The average thickness of the realized films used for evaluation of migration, radical and scavenging properties and for microscopic analysis were about 357.5 ± 10.5 µm and 206.1 ± 20.7 µm respectively. The final GA-PHBV films were stored in hermetically box free of oxygen until use.

2.3. Determination of the film properties

2.3.1. Evaluation of GA recovery and distribution in the film after thermoforming

2.3.1.1. From macroscopic point of view. PHBV/GA sheets of 144 cm² was divided into four equal parts and GA contained in each part was quantified after extraction, at 25 °C, during 18 h using methanol as solvent. The amount of GA was determined thanks to UV quantification in an Aquity UPLC (Waters, Milford, MA) liquid chromatography system, equipped with a photodiode array detector (DAD). The Waters column was 100 mm × 2.1 mm, HSS T3, with 1.8 µm particles size. Solvents used were A (99% H₂O and 1% HCOOH v/v) and B (80% CH₃CN, 19.9% H₂O and 0.1% HCOOH) with a flow rate of 0.55 mL/min. The gradient conditions were as follows: from 0 to 5 min, 99–60% A; from 5 min to 7 min, 60–1% A; from 7 min to 8 min, 1% A; from 8 min to 9 min, 1–99.9% A. The injection volume was 2 µL, DAD was set at 280 nm, and gallic acid was detected at 1.5 min retention time (Roumeas, Billerach, Aouf, Dubreucq, & Fulcrand, 2018). GA was quantified after external calibration with GA for standard dissolved in methanol.

2.3.1.2. From microscopic point of view. PHBV/GA films of 1 cm width and 200 µm thickness (thinner films were used for this analysis) were observed with a wide-field microscope Eclipse Ni-E (Nikon Instruments Inc, NY, USA) with filter cube UV-2A, exc: 330–380, em: 420–800. The pictures were obtained with the 10X Plan APO objective and a Nikon CMOS DS-Ri2 camera. They were processed with Image J v1.8.0 software.

2.3.2. GA migration into food simulants

Three food simulants were selected to study the GA migration, namely, simulant A (10% ethanol) corresponding to aqueous food, simulant D1 (50% ethanol) corresponding to alcoholic food (above 20% of alcohol) and oil in water emulsion and simulant D2 (vegetable oil was replaced by isooctane) corresponding to food containing free fats on the surface (European Standard EN 10/2011, (European Commission, 2011). Migration studies were conducted in triplicate at 25 °C over 10 days in a climatic chamber (Memmert, Germany). Double-sided, total immersion migration tests were performed with 60 cm² of films and 100 mL of each simulant (area-to-volume ratio around 6 dm²/L). A blank test for each simulant was also carried out. Extracts (1 mL) were collected each day and GA concentration in food simulant was quantified by UPLC, as previously mentioned in section 2.3.2.1.

To estimate the corresponding percentage of GA diffused in food simulant, the following equation was used:

$$\% \text{ of GA diffused in food simulant} = \frac{C_x \times V_{FS}}{m_f \times \%GA} \quad (1)$$

With, C_x the mass concentration of GA (mg/L), V_{FS} the volume of food simulant (L), m_f the mass of film (mg) and %GA the percentage of GA included in the PHBV film (5 wt%).

2.3.3. Radical scavenger activity of released GA into food simulants

The DPPH assay consists in measuring the ability of a molecule to reduce the 2,2-diphenyl-1-picryl-hydrazyl radical (DPPH) in methanol,

resulting in its bleaching at 517 nm. The scavenging activity of GA against DPPH was performed spectrometrically at 517 nm and 30 °C, according to (Laguna et al., 2020). Solutions containing 100 µL of each food simulant collected at each time (with GA concentrations from 8 to 54 mg/L) and 100 µL of DPPH methanolic solution (40 mg/L) were poured into Humidity cassette microplates (TEC96ft_cell Tecan 96Flat Transparent). The absorbance decay was monitored each 2 min until it reached a steady state (15 min). The spontaneous bleaching of DPPH was also measured in absence of antioxidant (blank). All the determinations were performed in duplicate. The percentage inhibition values (I%) were calculated using the following equation:

$$I\% = \frac{Abs_c - Abs_s}{Abs_c} \times 100 \quad (2)$$

where Abs_c is the absorbance of pure DPPH and Abs_s is the absorbance of the sample.

2.3.4. Oxygen scavenger properties of active component and active film

The oxygen scavenger capacity of the active mixture composed of GA and Na_2CO_3 in ratio 2:1 in both powder form and inclusion in polymer matrix was determined according to DIN 6139 at 23 °C and 100% RH (Pant et al., 2017). The active mixture (0.3 g of GA and 0.17 g of Na_2CO_3 for powder mixture or 5.8 g of film pieces containing 5% of GA and 2.5% of Na_2CO_3 for inclusion polymer matrix) were stored in hermetically closed glass cells ($V=514 \text{ cm}^3$) equipped with steel lid. The saturated humidity was assured by distilled water (50 mL) put in a glass bowl at the bottom of the cell. The O_2 depletion in the headspace (initial gas atmosphere: air) during storage was determined non-destructively using a luminescence-based oxygen detection system (PreSens Precision Sensing GmbH, Regensburg, Germany) with an optical sensor spot stuck on the underside of the cell wall. The O_2 partial pressure in the cell was monitored over time and the cell was briefly reopened to regenerate the oxygen at 20.9% when it became zero. The experiment conducted in triplicate, was stopped when the maximum absorption capacity was reached, i.e. when no decrease of oxygen partial pressure has been detected. The O_2 absorption quantity (mg O_2) was calculated from the O_2 partial pressure depletion, using the following equation:

$$m_{O_2} = \frac{P_{O_2} \times V_{HS} \times M_{O_2}}{R \times T} \quad (3)$$

Where m_{O_2} is the oxygen content absorbed into the system (g), $R=8.314 \text{ Pa m}^3 \text{ mol}^{-1} \text{ K}^{-1}$ is the gas ideal constant, T is the temperature (K), V_{HS} is the headspace volume of the cell (m^3) and M_{O_2} is the oxygen molar mass (g mol^{-1}). The oxygen absorption capacity of active compound film was calculated in mg of absorbed O_2 per gram of gallic acid.

2.3.5. Oxygen permeability of the active film

Active film (with $357.5 \pm 10.5 \mu\text{m}$ thickness) was cut into circles with 12.5 cm^2 diameter and their oxygen permeability ($\text{mol m}^{-1} \text{ s}^{-1} \text{ Pa}^{-1}$) was measured at 23 °C and 50% RH using an oxygen permeation cell (OTR, PresSens-GmbH, Germany) according to a modified ASTM Standard (2007) procedure. The oxygen partial pressure in the upper chamber was measured using an optical luminescence quenching method (Presens, GmbH).

The oxygen permeability coefficient PO_2 ($\text{mol m}^{-1} \text{ s}^{-1} \text{ Pa}^{-1}$) was determined as reported in the following equation:

$$PO_2 = \frac{\dot{P} \times l}{A \times P_{atm}} \quad (4)$$

Where \dot{P} (mol s^{-1}) is the slope of the oxygen partial pressure increase in the upper chamber, A (m^2) and l (m) are the surface and the average thickness of the film respectively. P_{atm} is the standard atmosphere pressure. The thickness of the film was determined at five different points of the film using a micrometer (Mitutoyo).

2.4. Mathematical models development

2.4.1. Modeling of the apparent diffusion of GA in the PHBV film

Assuming that: (i) the film is a one dimensional infinite plane sheet with an homogeneous thickness, (ii) GA is homogeneously distributed in the PHBV film and in food simulant (if GA diffused in food simulant) and (iii) the film does not swell during the process; the estimation of the gallic acid apparent diffusivity (D_{app}) in the PHBV film was made using an analytical solution of the Fick's second law (Eq. (5)) as described by Lajarrige, Gontard, Gaucel, Samson, and Peyron (2019).

$$\frac{M_t}{M_\infty} = 1 - \sum_{n=0}^{\infty} \frac{2\alpha}{1 + \alpha + \alpha^2 q_n^2} \exp\left\{-\frac{Dq_n^2 t}{L^2}\right\} \quad (5)$$

With

$$\alpha = \frac{1}{K_{P,F}} \frac{V_F}{V_P} \quad (6)$$

where: M_t is the total amount of GA in food simulant at time t and M_∞ is the total amount of GA in food simulant at the steady state, V_P is the polymer volume and V_F the food simulant volume, $(q_n)_n$, the positive roots of the equation $\tan q = -\alpha q$ and $K_{P,F}$, the partition coefficient of the additive in the polymer/food simulant system.

The numerical simulations were carried out using Matlab® software and its `lsqnonlin` function to estimate the D_{app} . For each model fitting, the quality of fit was estimated through the percentage of Root Mean Square Error (RMSE):

$$RMSE = \frac{1}{M_0} \sqrt{\frac{1}{N} \sum_{i=1}^N ((M_t)_{experimental} - (M_t)_{predicted})^2} \times 100 \quad (7)$$

Where M_0 is the initial mass of GA in the film and M_t is the mass of GA into a food simulant at time t .

2.4.2. Modeling of O_2 absorption by gallic acid

2.4.2.1. Reaction model for GA powder. The absorption kinetic was then depicted by an order 2 kinetic, as O_2 absorption depends on both scavenger and O_2 concentrations. As a simplification, partial orders were set to 1, leading to the following system of ODEs:

$$\frac{d[O_2]}{dt} = -nk[GA][O_2] \quad \frac{d[GA]}{dt} = -k[GA][O_2] \quad (8)$$

where $[O_2]$, is the concentration of O_2 in mol m^{-3} , $[GA]$ is the concentration of GA in mol m^{-3} , n is the apparent stoichiometric coefficient for oxidation of GA by O_2 (%); and k is the kinetic coefficient in $\text{m}^{-3} \text{ s}^{-1} \text{ mol}^{-1}$ for GA oxidation.

2.4.2.2. Reaction-diffusion model of GA introduced in PHBV film. A reaction-diffusion system, similar to the one developed by Kombaya-Touckia-Linin et al., (2019), was used to describe the oxygen absorption by GA embedded in the film. The model described the diffusion of O_2 into the polymer matrix using Fick's law of diffusion and the reaction between O_2 and GA according to the Eq. (8).

It was assumed that: (i) GA was immobile into the polymer matrix; (ii) an homogeneous distribution of GA inside the film structure was achieved; (iii) the polymer was considered as homogeneous material with a single, constant, apparent O₂ diffusivity D_{O₂} (m² s⁻¹).

The mathematical model for a plane film geometry reduced to the one-dimensional reaction–diffusion system is given in Eq. (9), for x ∈]–L/2, L/2, where L is the thickness of the film:

$$\frac{\partial [O_2]}{\partial t}(t, x) = D_{O_2} \frac{\partial^2 [O_2]}{\partial x^2} - kn[O_2](t, x)[GA](t, x) \frac{\partial [GA]}{\partial t}(t, x) = -k[O_2](t, x)[GA](t, x) \tag{9}$$

where k and n are the kinetic parameters previously determined for the powder.

The initial GA and O₂ concentrations, supposed uniform in the film were the following ones:

$$[GA](t_0) = \frac{x_{GA}^f \rho^f}{M_{GA}} [O_2](t_0) = 0 \tag{10}$$

Where x_{GA}^f represent the mass fraction of GA inside the active film (kilograms of gallic acid per kilogram of active film) ρ^f is the apparent density of PHBV (kg m⁻³) and M_{GA} is the molar mass of GA (kg mol⁻¹). It was assumed that [O₂](t₀) = 0.

The boundary conditions are similar to those described by Kom-baya-Touckia-Linin et al., (2019).

$$D_{O_2} \frac{\partial [O_2]}{\partial x}(t, x) = \frac{\varphi_{L/2}}{A} = \frac{\varphi_{-L/2}}{A} = \frac{k}{RT} \left(P_{O_2,HS} - \frac{[O_2](t, x)}{K_H} \right) at \quad x = (-) \frac{L}{2} \text{ and } \forall t \geq 0 \tag{11}$$

Where T (K) is the temperature, R the ideal gas constant, P_{O₂,HS} (Pa) and P_{O₂,His} (Pa) are the oxygen partial pressure in the headspace and at the vicinity of the composite surface, respectively.

In Eq. (11) the external mass transfer coefficient k are reported using Biot number (Bi).

$$k = \frac{2B_i D_{O_2}}{L} \tag{12}$$

For the mass balance of oxygen into headspace it was assumed that: (i) the film is isolated into a container with a constant headspace volume V_{HS} (m³) (ii) the gas flow is negligible through the container. Therefore, the variation of the oxygen partial pressure is calculated as below:

$$\frac{\partial P_{O_2, HS}}{\partial t} = k \frac{A}{V_{HS}} \left(2P_{O_2,HS} - \frac{[O_2](t, x = L/2)}{K_H} - \frac{[O_2](t, x = -L/2)}{K_H} \right) \tag{13}$$

Numerical simulation were performed with a biot number (Bi=10⁵). Eqs. (8) and (13) were transformed from a partial differential equation system into an ordinary differential equation (ODE) system by a spatial discretization with a second order central difference method and mesh of 100 nodes. The resulting ODE system was numerically solved using MATLAB (MathWorks).

3. Results and discussion

3.1. Impact of the thermoforming process on GA stability and distribution in PHBV film

PHBV/GA sheets were divided into four equal parts and GA contained in each part was quantified after extraction. It was observed that a

similar amount of GA (4.25 ± 0.16 g GA /100 g of film) was recovered from each part, indicating a good homogeneity of GA at the macromolecular level. However, the total amount of GA extracted from the film sheet was only 85 ± 3% of the initial amount introduced before the thermoforming process. Thus, the thermal process (3.5 min at 180 °C and cooling down in air) provoked 15% of GA mass loss, that could be attributed to thermal degradation, and more specifically to oxidation as no volatile compounds could be produced at this temperature (Alberti et al. 2016). Indeed, the thermal degradation of GA was already observed by Ahn et al., (2016) and quantified by Santos et al., (2012). This latest measured a GA degradation of 9% at temperature range between 68 °C and 213 °C.

The apparent homogeneity of GA in PHBV matrix has been challenged by wide field microscopy analysis. Images of the surface of the PHBV/GA films represented in Fig. 1 (Fig. 1B is a close-up of Fig. 1A)

clearly showed that at the microscopic scale, the fluorescent GA which emitted UV wave after excitation, appearing in yellow color; was not homogeneously distributed in the polymer matrix. Furthermore, the numerous bubbles present on the surface of the film could be attributed to the sodium carbonate that was not melted after film processing (tm = 850 °C). Some studies also reported heterogeneous dispersion of active compounds in polymer films, such as thymol or eugenol in LDPE (Krepker et al. 2017; Goñi, Gañán, Strumia, & Martini, 2016) or GA in chitosan (Ahn et al., 2016; Rui et al. 2017; Sun, Wang, Kadouh, & Zhou, 2014). This heterogeneity depends mainly on the GA concentration and nature of the interactions between the active compound and the polymer chains (Rui et al., 2017). Indeed, GA at low concentrations was able to form hydrogen bounds with polymer matrix; while at high concentrations a part of GA could remain unlinked, forming aggregates.

3.2. The antiradical activity of GA released into food simulants

The concentration and percentage (Eq. 1) of GA diffused from PHBV film into aqueous food simulant A and fatty food simulant D1 are shown in Fig. 2. In contrast, GA was not released in oily food simulant D2 (data not shown).

For both food simulants A and D1, the migration of GA increases with

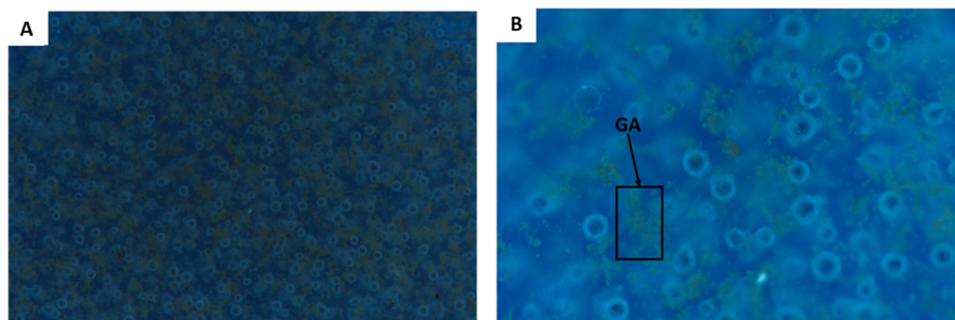


Fig. 1. Wide-field microscopy of PHBV-GA films of 1 cm width and 200 μm thickness, with 10X Plan APO objective. Image 1B is a close-up of image 1A.

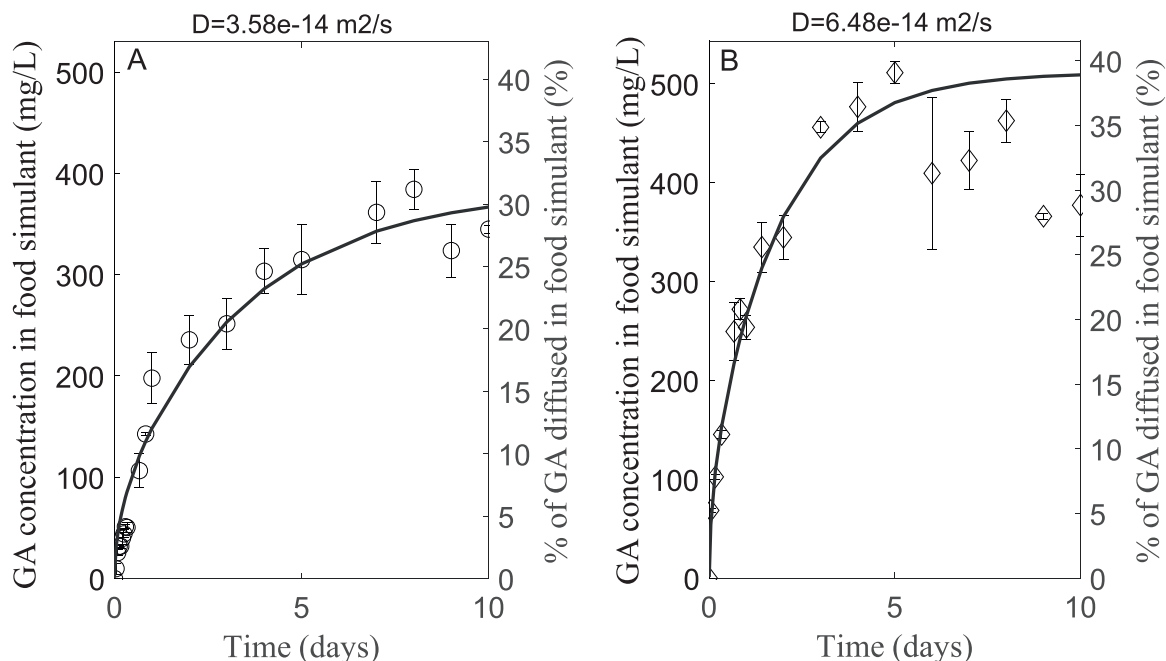


Fig. 2. Migration of GA (mg/mL or %) from PHBV film into food simulant A (10% ethanol) (A) and food simulant D1 (50% ethanol) (B) at 25 °C. Dots and line represented experimental data and model data respectively. The error bars represent the standard deviation (n = 3).

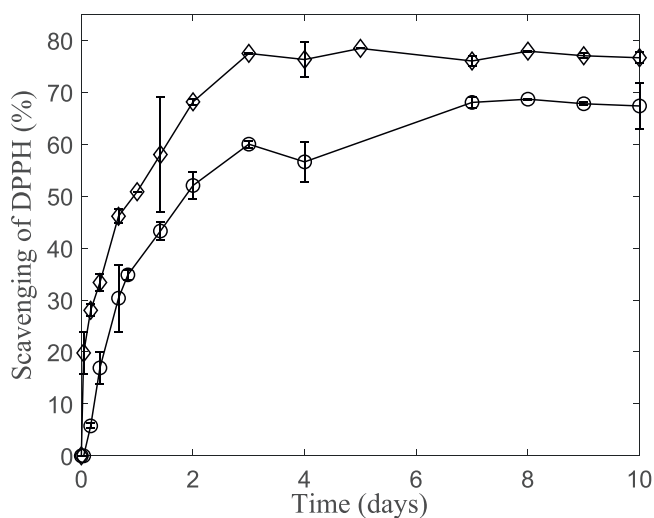


Fig. 3. Kinetic of DPPH radical scavenging activity after migration of GA in food simulant A, ie 10% ethanol (circle) and D1, ie 50% ethanol (diamond). The error bars represent the standard deviation (n = 2).

time and reaches a maximum, point after which there is a slight decrease of GA concentration in food simulants, as a result of oxidation of the GA diffused (combination of diffusion and oxidation, due to the solubilization of oxygen in food simulants) (Fig. 2). This oxidation lead to an underestimation of the GA diffused in food simulants. GA migration is higher in food simulants D1 (511 mg/L after 5 days, corresponding to 39% of the initial amount of GA present in the film) than in food simulant A (384 mg/L after 8 day, corresponding to 31% of the initial GA present in the film), likely due to the higher solubility of GA in ethanol compared to water (more than 30 times) (Daneshfar, Ghaziaskar, & Homayoun, 2008; Noubigh, Jeribi, Mgaidi, & Abderrabba, 2012). The same behaviour was observed for the migration of thymol which was proportional to the amount of ethanol in the simulant (Tawakkal, Cran, & Bigger, 2016). Therefore, the maximum release of GA is expected to occur in less polar foodstuffs, such as oil-in-water emulsions (sauces, dressings or high-fat dairy products) and /or alcoholic beverages.

This increase of GA release in ethanol-rich medium was confirmed by the value of adjusted apparent GA diffusivities in PHBV film, which is two time higher when the PHBV sheet is in contact with food simulant D1 ($6.48 \times 10^{-14} \text{ m}^2 \text{ s}^{-1}$) compared to food simulant A ($3.58 \times 10^{-14} \text{ m}^2 \text{ s}^{-1}$). The apparent diffusivity values identified for GA are in the same order of magnitude than those found in the literature for other low molecular weight constituents. For example, Rubilar, Cruz, Zuñiga,

Khmelninskii, and Vieira (2017) identified a GA diffusivity between 3.7×10^{-14} and $6.1 \times 10^{-14} \text{ m}^2 \text{ s}^{-1}$ from chitosan film into water using a Fickian model. An acceptable fitting was observed between experimental data and model with an average RMSE of 6.5% and 11.5% in food simulant A and D1 respectively. The difference between model and experimental data was higher for the longer times, because the diffusion of GA reached a plateau and oxidation that appeared during experiments was neglected in model.

The released GA into food simulants A and D1 displayed a significant inhibition of DPPH radical and as expected, is ascribed to the total amount of GA released into the simulant. As depicted in Fig. 3, at maximum release, the percentage inhibition value (%) was $68.7 \pm 0.1\%$ and $77.5 \pm 0.1\%$ in simulant A and D1 respectively. In the case of food represented by simulant D1, the protection of lipids against radical-induced oxidation would be effective. However, the antioxidant activity of GA may not be exploited if the maximum daily intake is not respected.

The amount of GA released in contact with food simulants D1 and A, after 10 days, was about $377 \pm 31 \text{ mg/L}$ and $344 \pm 4 \text{ mg/L}$ respectively (Fig. 2 A, B) (corresponding to around 30% of the initial GA present in the film), while the amount of GA released in simulant D2 (isooctane) was zero. Although no Admissible Daily Intake (ADI) was estimated for gallic acid, the regulation established the maximal acceptable ADI at 0.2 mg/kg of body weight for propyl gallate (a GA ester), corresponding to 14 mg for an adult with an average body weight of 70 kg (FAO/WHO expert, 1976). Assuming that GA would have a similar ADI value, the use of a conventional tray with 10 g weight (for 150 g of food) containing 5% of GA whose 30% diffuses in food after 10 days (simulants A and D1), will lead to the intake of 150 mg of GA for one adult (supposing he consumed all the food), so 10 times higher than acceptable ADI. However, when a conventional lid film with 1 g weight is used, 15 mg of GA would diffuse into food, which is equivalent to the maximal ADI. Consequently, the development of active material consisting of gallic acid should only be permitted in trays at a concentration lower than 0.5% or in lid film at a concentration lower than 5% for food corresponding to simulants A and D1.

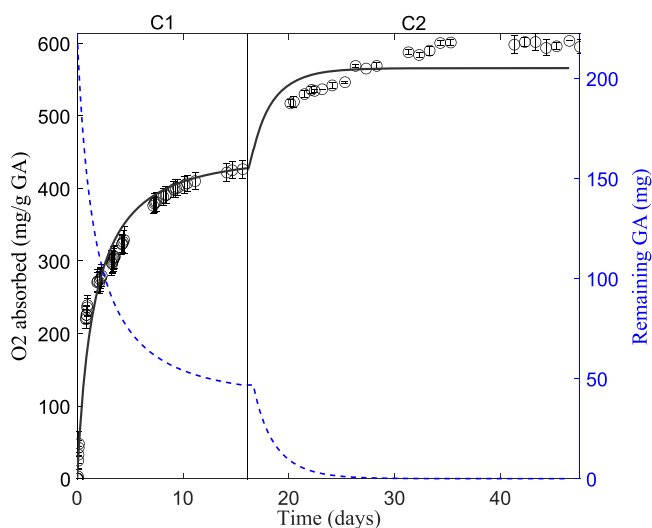


Fig. 4. Experimental (dots) and predicted (black line) O_2 absorption capacities of gallic acid / Na_2CO_3 powder (2:1) ($\text{mg O}_2/\text{g}$ of GA) at 23°C and 100% RH and predicted consumption rate of gallic acid / Na_2CO_3 powder (2:1) at the same condition (blue dotted line). Between cycle 1 (C1) and cycle 2 (C2), the jar was reopened to recharge the headspace in oxygen. The error bars represent the standard deviation ($n = 3$).

3.3. Oxygen absorption properties of the active PHBV film

3.3.1. Oxygen absorption capacities of GA/ Na_2CO_3 powder

The experimental kinetic of O_2 absorption capacity of the GA / Na_2CO_3 powder (2:1) at 23°C and 100% RH and the corresponding, calculated remaining active GA is displayed in Fig. 4. After 15 days the cell was reopened in order to refill the headspace with oxygen, which is reflected by the two cycles present in the figure. A maximal absorption capacity of $595 \text{ mg O}_2 \text{ g}^{-1}$ of GA was reached in 30 days. Indeed, in basic conditions, GA is indirectly a good oxygen scavenger because it has the capacity to donate four acidic protons and to form several forms of gallate radicals by consuming molecular oxygen (Pant et al., 2019). This maximal absorption capacity is slightly higher than the O_2 absorption capacity of 447 mg O_2 absorbed/ g of GA measured by Pant et al., (2017) using the same mixture composition at 21°C and 100% RH.

The mathematical model showed a good fitting performance to experimental data with a RMSE of $21.9 \text{ mg O}_2 \text{ g}^{-1}$ of GA. Table 1 showed the estimated values of kinetic coefficient k ($7.8 \times 10^{-7} \text{ m}^3 \text{ mol}^{-1} \text{ s}^{-1}$) and stoichiometric coefficient n (3.57). These parameter values are close to those found by (Pant et al., 2019) that used the same model on GA/ Na_2CO_3 powder (2:1) with a kinetic coefficient k of $1.496 \times 10^{-6} \text{ m}^3 \text{ mol}^{-1} \text{ s}^{-1}$ and a stoichiometric coefficient n of 2.53.

3.3.2. Oxygen absorption capacities of active film

The kinetic of O_2 absorption capacity of the GA / Na_2CO_3 (2:1) incorporated in PHBV film at 23°C and 100% RH and the calculated remaining active GA in film is reported in Fig. 5. GA in PHBV film reached approximately the same maximal absorption capacity as in powder form, with an average value of $581 \text{ mg O}_2 \text{ g}^{-1}$ of GA. However, it took three times as long to reach this maximal absorption capacity (around 100 days for the film versus 30 days for the powder). Indeed, in the experiment with activated powder oxygen is directly in contact with GA, while in the PHBV/GA film, it must first be absorbed in the polymer matrix and then diffused into the polymer to reach GA, which consequently slows down its absorption kinetics. The diffusion-reaction mechanism is clearly O_2 diffusion rate-limiting.

The mathematical model used to simulate the oxygen absorption by GA present in the PHBV film integrated both: (i) the sorption and diffusion of oxygen in the PHBV film (diffusion part of the model) and (ii) the absorption kinetic of GA (reaction part of the model) (Eq. 9). Assuming that absorption kinetic of GA in its two forms (powder or embedded in film) is similar, the kinetic (k) and stoichiometric (n) coefficients of the GA powder were used, i.e. $7.8 \times 10^{-7} \text{ m}^3 \text{ mol}^{-1} \text{ s}^{-1}$ and 3.57 respectively. In literature, the diffusivity value of oxygen D_{O_2} in PHBV, or PHB ranges from 1.2×10^{-13} to $1.1 \times 10^{-12} \text{ m}^2 \text{ s}^{-1}$ (Crétois, Follain, Dargent, Soulestin, & Bourbigot, 2014; Gupta, Mulchandani, Shah, Kumar, & Katiyar, 2018). To estimate the sorption of oxygen S_{O_2} (or k_h) in PHBV film, the permeability of the film was measured, its value being $1.34 \times 10^{-17} \pm 1.66 \times 10^{-18} \text{ mol m}^{-1} \text{ s}^{-1} \text{ Pa}^{-1}$ (Table 1), the S_{O_2} was estimated by the relation $\text{S}=\text{P}/\text{D}$. It ranged from 1.1×10^{-4} to $1.2 \times 10^{-5} \text{ mol m}^{-3} \text{ Pa}^{-1}$ depending on the D value considered with the range found in literature. It was observed that for a same P_{O_2} value (here $1.34 \times 10^{-17} \text{ mol m}^{-1} \text{ s}^{-1} \text{ Pa}^{-1}$) the oxygen absorption kinetic strongly depends on the couple of D_{O_2} and S_{O_2} used (Fig. 5). For example, on the first replica, the couple $\text{D}_{\text{O}_2} = 1.2 \times 10^{-13} \text{ m}^2 \text{ s}^{-1}$ and $\text{S}_{\text{O}_2} = 1.1 \times 10^{-4} \text{ mol m}^{-3} \text{ Pa}^{-1}$ allowed to reach an absorption capacity of $346 \text{ mg O}_2 \text{ g}^{-1}$ of GA after 123 days, while the couple $\text{D}_{\text{O}_2} = 1.1 \times 10^{-12} \text{ m}^2 \text{ s}^{-1}$ and $\text{S}_{\text{O}_2} = 1.2 \times 10^{-5} \text{ mol m}^{-3} \text{ Pa}^{-1}$ allowed to reach an absorption capacity of $211 \text{ mg O}_2 \text{ g}^{-1}$ of GA after 123 days (39% less than the previous case) (Fig. 5). This result is highlighting the importance to well determine both diffusivity and solubility values of oxygen into PHBV to well predict the evolution of oxygen in active packaging headspace.

The model did not fit the experimental data for both replicates (Fig. 5, $\text{P}_{\text{O}_2} = 1.34 \times 10^{-17} \text{ mol m}^{-1} \text{ s}^{-1} \text{ Pa}^{-1}$), probably because of the modification of gas permeability due to the lack of active compound

Table 1Values of parameters used in the oxygen absorption capacity model of PHBV containing 5% of GA and 2.5% of Na₂CO₃ film.

O ₂ absorption by gallic acid					
Sample	k (m ³ mol ⁻¹ s ⁻¹)	n	Conditions	Reference	
GA/Na ₂ CO ₃ powder in ratio 2:1	7.8 × 10 ⁻⁷	3.87	23 °C and 100% RH	This study	
O ₂ barrier properties of PHBV					
Sample	Permeability (mol m ⁻¹ s ⁻¹ Pa ⁻¹)	Diffusivity (m ² s ⁻¹)	Solubility (mol m ⁻³ Pa ⁻¹)	Conditions	Reference
PHBV	1.34 × 10 ⁻¹⁷	–	Estimated from S=P × D= 1.12 × 10 ⁻⁴	23 °C and 50% RH	This study
PHBV	Not use	1.2 × 10 ⁻¹³		23 °C and 0% RH	Crétois et al., 2014
PHB	Not use	1.1 × 10 ⁻¹²	Estimated from S=P × D= 1.22 × 10 ⁻⁵	24 °C and 80% RH	(Sanchez-Garcia, Gimenez, & Lagaron, 2008)

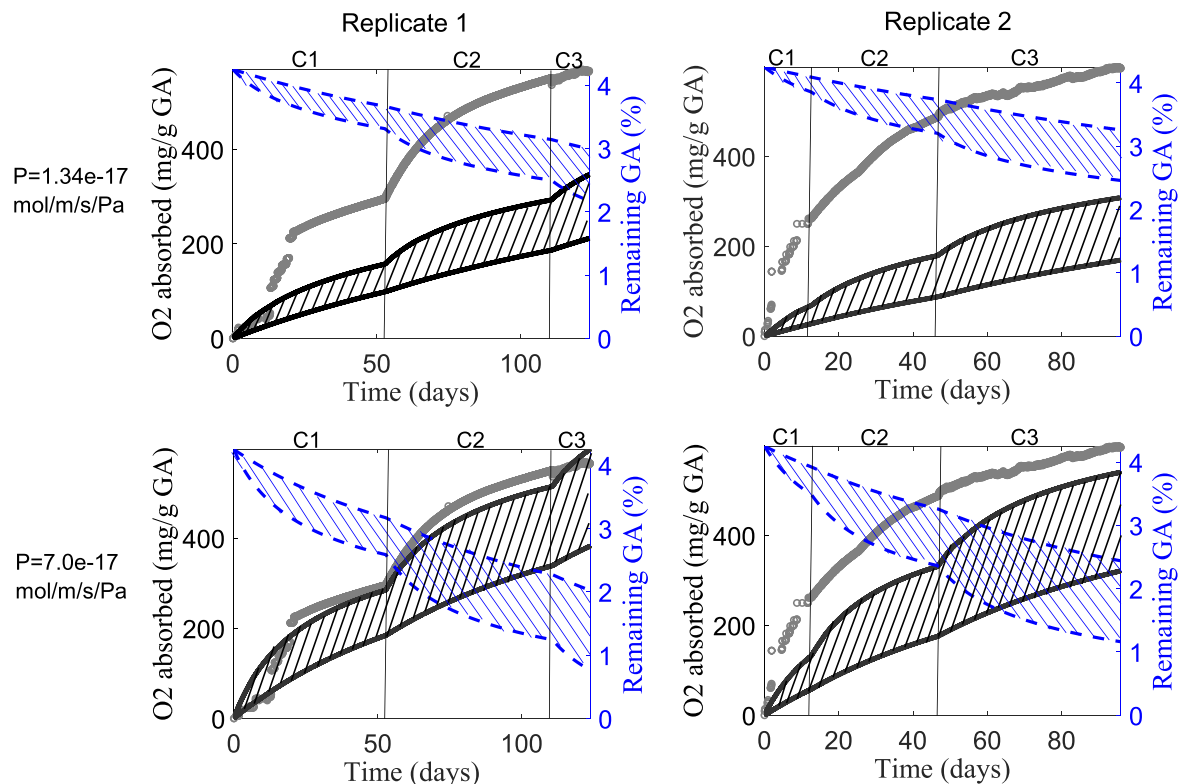


Fig. 5. Experimental (dots) and predicted (black line) O₂ absorption capacities of PHBV/GA(5%)/ Na₂CO₃(2.5%) film at 21° and 100% RH; and predicted consumption rate of the film at the same condition (blue dotted line) for two replicates (one at right and one at left) and with two different values of O₂ permeability (1.34 × 10⁻¹⁷ mol/m/s/Pa up and 7.0 × 10⁻¹⁷ mol/m/s/Pa down). For each P_{O₂} value, two couple of D_{O₂} and S_{O₂} in PHBV film were tested to represent the predicted absorption capacities (black line) that were joined by cross hatch. Between cycle 1 (C1) and cycle 2 (C2); and between cycle 2 (C2) and cycle 3 (C3), the jar was reopened to recharge the headspace in oxygen. (For interpretation of the references to colour in this figure, the reader is referred to the web version of this article.)

homogeneity in the PHBV film (confirmed by microscopy analysis- Fig. 1). The permeability of PHBV film containing exhausted active compounds (5 wt% of GA and 2.5 wt% of Na₂CO₃) was measured. Unfortunately, measurement was unexploitable because of exceeded quantification threshold. The excessively high oxygen increase during the permeability measurement confirms the presence of pores in the active PHBV film. These results correlate with Ahn's observations (Ahn et al., 2016) that the increase in GA/potassium carbonate from 1% to 20% in LDPE induces a reduction of the intermolecular force between polymer chains, leading to the apparition of pores, and consequently to the increase of gases permeability.

The oxygen permeability values of PHBV in litterature usually range from 1 to 7 × 10⁻¹⁷ mol m⁻¹s⁻¹ Pa⁻¹ (Berthet, Angellier-Coussy, Guillard, & Gontard, 2016). In a last trial, the model simulating the oxygen

absorption of GA in PHBV film was run with the upper limit of this P_{O₂} range, i.e. with the value of 7 × 10⁻¹⁷ mol m⁻¹ s⁻¹ Pa⁻¹, so 7 times higher than that measured in this study (with a S_{O₂} range from 1.1 × 10⁻⁴ to 1.2 × 10⁻⁵ mol m⁻³ Pa⁻¹ and a D_{O₂} range from 5.9 × 10⁻¹² to 6.3 × 10⁻¹³ mol m⁻³ Pa⁻¹). With this new permeability value, the model fitted the experimental data for the first replica with the couple D_{O₂} = 6.3 × 10⁻¹³ m² s⁻¹ and S_{O₂} = 1.1 × 10⁻⁴ mol m⁻³ Pa⁻¹. The same couple of parameters also allowed to well reflect the experimental kinetic of cycle 2 and 3 for the second replica, the gap of 120 mg O₂ g⁻¹ GA between experimental data and model accumulated in cycle 1, being maintained in the two following cycles. Therefore, these observations highlight that further research is needed to better understand and predict the absorption of oxygen by activated GA in polymer matrix.

4. Conclusion and recommendations for the use of PHBV/GA film as food packaging

In this study, active film based on PHBV/activated GA was developed. This film showed a promising capacity as both radical and oxygen scavenger and could be used as biodegradable packaging for different kinds of food.

In the case of contact with aqueous and some fatty food (food simulant A and D1) as meat, fish, or cheese, the GA amount present in the packaging should be lower than 0.5% in trays and could reach 5% in lid film, in the case of a food of 150 g (154 mL) packed in a 10 g active tray (443 mL, of which 289 mL of headspace) with 418 cm² of surface and 1 g lid film with 256 cm² of surface. GA which does not diffuse into food could act as oxygen absorber, with an oxygen absorption capacity of 120 mg O₂ g⁻¹ of GA after 10 days, corresponding to 7.7% of oxygen g⁻¹ of GA for a volume of 289 mL. This oxygen absorption capacity could limit the oxygen entrance through the packaging and would enhance the benefit of oxygen-free modified atmosphere packaging by strengthening food protection against oxidation.

Since the GA does not diffuse into vegetable oil (food simulant D2, replaced by isooctane in this study), no restriction on the amount of GA in the packaging applied for this type of food application. In this case, the protection from oxidation would be performed thanks to the oxygen absorption capacity of GA.

However, some improvements are still needed to find the right compromise between the amount of GA needed for effective antioxidant activity and maintaining the structural integrity of the film.

CRedit authorship contribution statement

FG, FC, CA, and VG conceived and designed the experiments. FG, and FC performed the experiments. FG, FC, CA, VG and ET analysed the data and wrote the paper. ET supervised the work. The authors thank Geneviève Conéjéro, the responsible for MRI-PHIV Platform at CIRAD for microscopy analyses.

Declaration of Competing Interest

The authors declare that they have no known competing financial interests or personal relationships that could influence the work reported in this paper.

Funding sources

The authors acknowledge the financial support by the Ministry of Education University and Research (MIUR) in the frame of the National Operational Program ESF-ERDF Research and Innovation 2014-2020, action I.1. Innovative PhD with industrial characterization.

References

- Ahn, B. J., Gaikwad, K. K., & Lee, Y. S. (2016). Characterization and properties of LDPE film with gallic-acid-based oxygen scavenging system useful as a functional packaging material. *Journal of Applied Polymer Science*, 133(43), 1–8. <https://doi.org/10.1002/app.44138>
- Alberti, A., Granato, D., Nogueira, A., Mafra, L. I., Colman, T. A. D., & Schnitzler, E. (2016). Modelling the thermal decomposition of 3, 4, 5-trihydroxybenzoic acid using ordinary least square regression. *International Food Research Journal*, 23, 30.
- Angellier-Coussy, H., Guillard, V., Guillaume, C., & Gontard, N. (2013). Role of packaging in the smorgasbord of action for sustainable food consumption. *Agro Food Industry Hi-Tech*, 24(3).
- Aydogdu, A., Yildiz, E., Aydogdu, Y., Sumnu, G., Sahin, S., & Ayhan, Z. (2019). Enhancing oxidative stability of walnuts by using gallic acid loaded lentil flour based electrospun nanofibers as active packaging material. *Food Hydrocolloids*, 95, 245–255. <https://doi.org/10.1016/j.foodhyd.2019.04.020>
- Berthet, M. A., Angellier-Coussy, H., Chea, V., Guillard, V., Gastaldi, E., & Gontard, N. (2015). Sustainable food packaging: Valorising wheat straw fibres for tuning PHBV-based composites properties. *Composites Part A Applied Science and Manufacturing*, 72, 139–147. <https://doi.org/10.1016/j.compositesa.2015.02.006>

- Berthet, M.-A., Angellier-Coussy, H., Guillard, V., & Gontard, N. (2016). Vegetal fiber-based biocomposites: Which stakes for food packaging applications? *Journal of Applied Polymer Science*. <https://doi.org/10.1002/app.42528>
- Bossu, J., Angellier-Coussy, H., Totee, C., Matos, M., Reis, M., & Guillard, V. (2020). Effect of the molecular structure of Poly(3-hydroxybutyrate-co-3-hydroxyvalerate) (P(3HB-3HV)) produced from mixed bacterial cultures on its crystallization and mechanical properties. *Biomacromolecules*, 21(4709–4723). <https://doi.org/10.1021/acs.biomac.0c00826>
- Campo, M., Pinelli, P., & Romani, A. (2016). Hydrolyzable tannins from sweet chestnut fractions obtained by a sustainable and eco-friendly industrial process. *Natural Product Communications*, 11(3), 409–415. <https://doi.org/10.1177/1934578x1601100323>
- Carrizo, D., Tabora, G., Nerin, C., & Bosetti, O. (2016). Extension of shelf life of two fatty foods using a new antioxidant multilayer packaging containing green tea extract. *Innovative Food Science and Emerging Technologies*, 33, 534–541. <https://doi.org/10.1016/j.ifset.2015.10.018>
- Cazón, P., Velazquez, G., Ramírez, J. A., & Vázquez, M. (2017). Polysaccharide-based films and coatings for food packaging: A review. *Food Hydrocolloids*, 68, 136–148. <https://doi.org/10.1016/j.foodhyd.2016.09.009>
- Coffigniez, F., Matar, C., Gaucel, S., Gontard, N., & Guilbert, S. (2021). The use of modeling tools to better evaluate the packaging benefits on our environment. *Front. Sustain. Food Syst.*, 5. <https://doi.org/10.3389/fsufs.2021.634038>
- Crétois, R., Follain, N., Dargent, E., Soulestin, J., & Bourbigot, S. (2014). Microstructure and barrier properties of PHBV / organoclays bionanocomposites. *Journal of Membrane Science*, 467, 56–66. <https://doi.org/10.1016/j.memsci.2014.05.015>
- Daneshfar, A., Ghaziaskar, H. S., & Homayoun, N. (2008). Solubility of gallic acid in methanol, ethanol, water, and ethyl acetate. *Journal of Chemical and Engineering Data*, 53(3), 776–778. <https://doi.org/10.1021/jc700633w>
- European Commission. (2011). Commission regulation (EU) No 10/2011. Of 14 January 2011 on plastic materials and articles intended to come into contact with food. *Official Journal of the European Union*, (L 12), 1–89.
- FAO/WHO expert committee on Food Additives, Food and Agriculture Organization of the United Nations and World Health Organization (1976). Toxicological evaluation of certain food additives.
- Gómez-Estaca, J., López-de-Dicastillo, C., Hernández-Muñoz, P., Catalá, R., & Gavara, R. (2014). Advances in antioxidant active food packaging. *Trends in Food Science and Technology*, 35(1), 42–51. <https://doi.org/10.1016/j.tifs.2013.10.008>
- Goñi, M. L., Gañán, N. A., Strumia, M. C., & Martini, R. E. (2016). Eugenol-loaded LLDPE films with antioxidant activity by supercritical carbon dioxide impregnation. *Journal of Supercritical Fluids*, 111, 28–35. <https://doi.org/10.1016/j.supflu.2016.01.012>
- Guillard, V., Gaucel, S., Fornaciari, C., Angellier-Coussy, H., Buche, P., & Gontard, N. (2018). The next generation of sustainable food packaging to preserve our environment in a circular economy context. *Frontiers in Nutrition*, 5, 1–13. <https://doi.org/10.3389/fnut.2018.00121>
- Gupta, A., Mulchandani, N., Shah, M., Kumar, S., & Katiyar, V. (2018). Functionalized chitosan mediated stereocomplexation of poly(lactic acid): Influence on crystallization, oxygen permeability, wettability and biocompatibility behavior. *Polymer*, 142, 196–208. <https://doi.org/10.1016/j.polymer.2017.12.064>
- Hellwig, M. (2019). The chemistry of protein oxidation in food. *Angewandte Chemie - International Edition*, 58(47), 16742–16763. <https://doi.org/10.1002/anie.201814144>
- Kombaya-Touckia-Linin, E. M., Gaucel, S., Sougrati, M. T., Stievano, L., Gontard, N., & Guillard, V. (2019). Elaboration and characterization of active films containing iron-montmorillonite nanocomposites for O₂ scavenging. *Nanomaterials*, 9(9). <https://doi.org/10.3390/nano9091193>
- Krepker, M., Shemesh, R., Danin Poleg, Y., Kashi, Y., Vaxman, A., & Segal, E. (2017). Active food packaging films with synergistic antimicrobial activity. *Food Control*, 76, 117–126. <https://doi.org/10.1016/j.foodcont.2017.01.014>
- Laguna, O., Durand, E., Baréa, B., Daugeat, S., Fine, F., Villeneuve, P., & Lecomte, J. (2020). Synthesis and evaluation of antioxidant activities of novel hydroxyalkyl esters and bis-aryl esters based on sinapic and caffeic acids. *Journal of Agricultural and Food Chemistry*, 68(35), 9308–9318. <https://doi.org/10.1021/acs.jafc.0c03711>
- Lajarrige, A., Gontard, N., Gaucel, S., Samson, M. F., & Peyron, S. (2019). The mixed impact of nanoclays on the apparent diffusion coefficient of additives in biodegradable polymers in contact with food. *Applied Clay Science*, 180, Article 105170. <https://doi.org/10.1016/j.clay.2019.105170>
- Licciardello, F., Wittenauer, J., Saengerlaub, S., Reinelt, M., & Stramm, C. (2015). Rapid assessment of the effectiveness of antioxidant active packaging-study with grape pomace and olive leaf extracts. *Food Packaging and Shelf Life*, 6, 1–6. <https://doi.org/10.1016/j.foodps.2015.08.001>
- Luzi, F., Pannucci, E., Santi, L., Kenny, J. M., Torre, L., Bernini, R., & Puglia, D. (2019). Gallic acid and quercetin as intelligent and active ingredients in poly(vinyl alcohol) films for food packaging. *Polymers*, 11(12). <https://doi.org/10.3390/polym11121999>
- Mohamed, S. A. A., El-Sakhawy, M., & El-Sakhawy, M. A. M. (2020). Polysaccharides, protein and lipid -based natural edible films in food packaging. *A Review. Carbohydrate Polymers*, 238, Article 116178. <https://doi.org/10.1016/j.carbpol.2020.116178>
- Noubigh, A., Jeribi, C., Mgaidi, A., & Abderrabba, M. (2012). Solubility of gallic acid in liquid mixtures of (ethanol + water) from (293.15 to 318.15) K. *Journal of Chemical Thermodynamics*, 55, 75–78. <https://doi.org/10.1016/j.jct.2012.06.022>
- Pant, A. F., Özkasikci, D., Fürtauer, S., & Reinelt, M. (2019). The effect of deprotonation on the reaction kinetics of an oxygen scavenger based on gallic acid. 7, 1–7. <https://doi.org/10.3389/fchem.2019.00680>

- Pant, A. F., Sangerlaub, S., & Muller, K. (2017). Gallic acid as an oxygen scavenger in bio-based multilayer packaging films. *Materials*, 10(489). <https://doi.org/10.3390/ma10050489>
- Radi, M., Firouzi, E., Akhavan, H., & Amiri, S. (2017). Effect of gelatin-based edible coatings incorporated with Aloe vera and black and green tea extracts on the shelf life of fresh-cut oranges. *Journal of Food Quality*, 2017. <https://doi.org/10.1155/2017/9764650>
- Roumeas, L., Billerach, G., Aouf, C., Dubreucq, E., & Fulcrand, H. (2018). Furfylated flavonoids: Fully biobased building blocks produced by condensed tannins depolymerization. *ACS Sustainable Chemistry and Engineering*, 6(1), 1112–1120. <https://doi.org/10.1021/acssuschemeng.7b03409>
- Rubilar, J. F., Cruz, R. M. S., Zuniga, R. N., Khmelinskii, I., & Vieira, M. C. (2017). Mathematical modeling of gallic acid release from chitosan films with grape seed extract and carvacrol. *International Journal of Biological Macromolecules*, 104, 197–203. <https://doi.org/10.1016/j.ijbiomac.2017.05.187>
- Rui, L., Xie, M., Hu, B., Zhou, L., Yin, D., & Zeng, X. (2017). A comparative study on chitosan/gelatin composite films with conjugated or incorporated gallic acid. *Carbohydrate Polymers*, 173, 473–481. <https://doi.org/10.1016/j.carbpol.2017.05.072>
- Sanches-Silva, A., Costa, D., Albuquerque, T. G., Buonocore, G. G., Ramos, F., Castilho, M. C., & Costa, H. S. (2014). Trends in the use of natural antioxidants in active food packaging: a review. Food additives and contaminants - part a chemistry, analysis. *Control, Exposure and Risk Assessment*, 31(3), 374–395. <https://doi.org/10.1080/19440049.2013.879215>
- Sanchez-Garcia, M. D., Gimenez, E., & Lagaron, J. M. (2008). Morphology and barrier properties of solvent cast composites of thermoplastic biopolymers and purified cellulose fibers. *Carbohydrate Polymers*, 71, 235–244.
- Santos, N. A., Cordeiro, A. M. T. M., Damasceno, S. S., Aguiar, R. T., Rosenhaim, R., Carvalho Filho, J. R., & Souza, A. G. (2012). Commercial antioxidants and thermal stability evaluations. *Fuel*, 97, 638–643. <https://doi.org/10.1016/j.fuel.2012.01.074>
- Singh, G., Singh, S., Kumar, B., & Gaikwad, K. K. (2020). Active barrier chitosan films containing gallic acid based oxygen scavenger. *Journal of Food Measurement and Characterization*, (0123456789)<https://doi.org/10.1007/s11694-020-00669-w>
- Sun, X., Wang, Z., Kadouh, H., & Zhou, K. (2014). The antimicrobial, mechanical, physical and structural properties of chitosan-gallic acid films. *LWT - Food Science and Technology*, 57(1), 83–89. <https://doi.org/10.1016/j.lwt.2013.11.037>
- Tawakkal, I. S. M. A., Cran, M. J., & Bigger, S. W. (2016). Release of thymol from poly (lactic acid)-based antimicrobial films containing kenaf fibres as natural filler. *LWT - Food Science and Technology*, 66, 629–637. <https://doi.org/10.1016/j.lwt.2015.11.011>
- Vermeiren, L., Devlieghere, F., Van Beest, M., De Kruijf, N., & Debevere, J. (1999). Developments in the active packaging of foods. *Trends in Food Science and Technology*, 10(3), 77–86. [https://doi.org/10.1016/S0924-2244\(99\)00032-1](https://doi.org/10.1016/S0924-2244(99)00032-1)
- Wang, Y., Du, H., Xie, M., Ma, G., Yang, W., Hu, Q., & Pei, F. (2019). Characterization of the physical properties and biological activity of chitosan films grafted with gallic acid and caffeic acid: A comparison study. *Food Packaging and Shelf Life*, 22. <https://doi.org/10.1016/j.fpsl.2019.100401>
- Wanner, G.T., 2010. O2 -zehrende und -anzeigende Packstoffe fur Lebensmittelverpackungen. Technische Universitat Munich.